ACS APPLIED MATERIALS & INTERFACES

www.acsami.org

Research Article

Polycationic HA/CpG Nanoparticles Induce Cross-Protective Influenza Immunity in Mice

Chunhong Dong, Ye Wang, Wandi Zhu, Yao Ma, Joo Kim, Lai Wei, Gilbert X. Gonzalez, and Bao-Zhong Wang*

Cite This: *ACS Appl. Mater. Interfaces* 2022, 14, 6331−6342

Read Online

ACCESS | Metrics & More | Article Recommendations | Supporting Information

ABSTRACT: The intranasal (i.n.) route is an ideal vaccination approach for infectious respiratory diseases like influenza. Polycationic polyethylenimine (PEI) could form nanoscale complexes with negatively charged viral glycoproteins. Here we fabricated PEI-hemagglutinin (HA) and PEI-HA/CpG nanoparticles and investigated their immune responses and protective efficacies with an i.n. vaccination regimen in mice. Our results revealed that the nanoparticles significantly enhanced HA immunogenicity, providing heterologous cross-protection. The conserved HA stalk region induced substantial antibodies in the nanoparticle immunization groups. In contrast to the Th2-biased, IgG1-dominant antibody response generated by PEI-HA nanoparticles, PEI-HA/CpG nanoparticles generated more robust and balanced IgG1/IgG2a antibody responses with augmented neutralization activity and Fc-mediated antibody-dependent cellular cytotoxicity (ADCC). PEI-HA/CpG nanoparticles also induced enhanced local and systemic cellular immune responses. These immune responses did not decay over six months of observation postimmunization. PEI and CpG synergized these comprehensive immune responses. Thus, the PEI-HA/CpG nanoparticle is a potential cross-protective influenza vaccine candidate. Polycationic PEI nanoplatforms merit future development into mucosal vaccine systems.

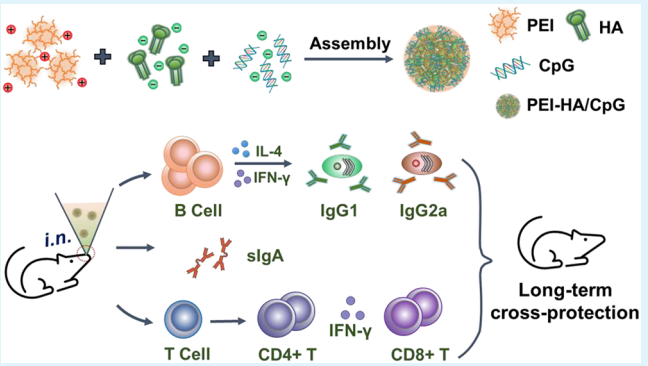

KEYWORDS: *influenza vaccine, intranasal vaccination, polyethylenimine, recombinant protein vaccine, cross-protection*

INTRODUCTION

Influenza viruses cause an enormous health and economic burden worldwide through seasonal, regional, and global outbreaks.[1] Seasonal influenza vaccines generally induce narrow immune responses that rapidly wane, leaving populations vulnerable to novel influenza strains. Advancements in influenza vaccine technology are needed to protect against a wide range of different viruses. Intranasal (i.n.) vaccination is a technology that can improve local mucosal immune responses beyond systemic immunity to vaccines. Local mucosal immunity can prevent heterologous and heterosubtypic influenza infection at the portal of virus entry.[2−4]

Recombinant protein vaccines have attracted enormous attention in influenza research due to their safety profile, rapid and egg-free production, and scalable manufacturing processes.[5,6] Most experimental or licensed influenza recombinant protein vaccines focused on hemagglutinin (HA) as the primary immunogen.[7,8] However, HA-induced immunity usually targets the immunodominant and variable HA head domain and is therefore strain specific. Moreover, intranasally administered protein antigens are generally less immunogenic, necessitating adjuvants for highly efficient intranasal protein vaccines. Adjuvants can enhance and manipulate immune responses in both scope and scale, thus improving protection potency and breadth. Subunit protein vaccination and live influenza virus infection generally induce different profiles of immune responses—Th2-dominant antibody responses or Th1 cellular responses, respectively.[9,10] Th1 responses facilitate more rapid recovery, particularly after distantly related heterologous viral challenges where cross-reactive neutralizing antibodies are rare.[11] Optimally, effective influenza vaccines require comprehensive Th1 and Th2 immune responses.

Nanoparticle vaccine platforms are one of the most encouraging adjuvant platforms due to their multiple intriguing advantages, including virus-mimicking sizes, simultaneous antigen and adjuvant delivery, inherent immunoenhancing effects, and high flexibility and versatility for various vaccine components.[6,12−14] Different nanoparticle formulations have

Received: October 5, 2021
Accepted: December 20, 2021
Published: January 27, 2022

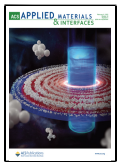

https://doi.org/10.1021/acsami.1c19192
ACS Appl. Mater. Interfaces 2022, 14, 6331−6342

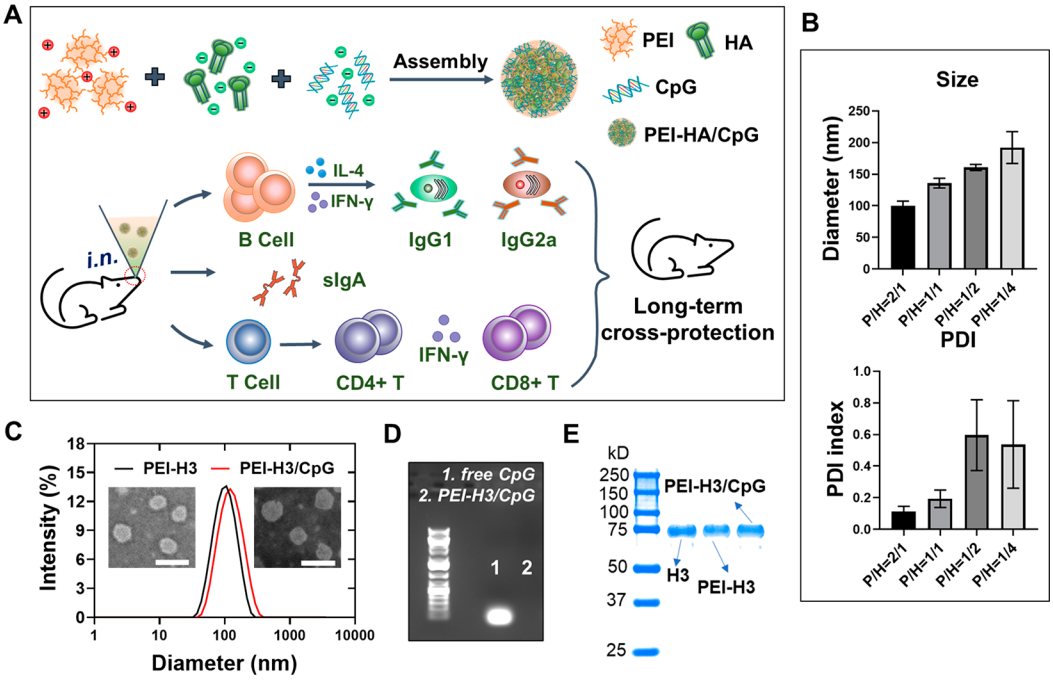

Figure 1. PEI-HA/CpG nanoparticle preparation for cross-protective influenza immunity. (A) Schematic illustration of the PEI-HA/CpG nanoparticle preparation and the induced immune responses. (B) Size and polydispersity index (PDI) of the PEI-H3 nanoparticles prepared at different PEI/H3 (P/H) ratios. (C) Size distribution and morphology of the PEI-H3 and PEI-H3/CpG nanoparticles (P/H = 2:1) characterized by DLS and TEM. (D) Determination of free CpG in PEI-H3/CpG nanoparticles by agarose gel electrophoresis. (E) Coomassie blue staining of SDS-PAGE.

shown immunoenhancing properties to improve immune responses, including polymeric nanoparticles,[15,16] virus-like particles,[17,18] carbon nanomaterials,[19,20] gold nanoparticles,[21−23] and lipid nanoparticles.[24] Moreover, in addition to their self-adjuvant effects, nanoparticle platforms can incorporate additional molecular adjuvants to generate complementary and synergistic adjuvant effects.

Cationic polymer polyethylenimine (PEI) can electrostatically complex with many biological macromolecules, enabling precise loading of antigen−adjuvant combinations in nanoparticles.[25] The assembled PEI−protein nanoparticle fabrication process is more straightforward, facile, rapid, and protein friendly than most nanoparticle formulations. Studies have indicated that PEI could potently increase the immunogenicity of DNA and protein vaccines.[25,26] However, PEI-induced immunity is Th2-dominant, like most other damage-associated molecular pattern (DAMP) adjuvants like aluminum hydroxide (Alum).[27] PEI failed to induce protective cellular responses, including cytotoxic T-lymphocyte (CTL), due to a lack of IFN-γ cytokine induction.[26] The PEI-adjuvanted subunit H1N1 HA protein protected mice against homologous influenza virus infection.[26] However, the adjuvant effect on cross protection against variant strains has not been investigated. The frequent antigenic mutations and reassortments of the influenza viruses necessitate the development of vaccines with cross protection.[28]

The coincorporation of molecular adjuvants with immunogens into nanoparticle platforms has been demonstrated to be a promising strategy for tailoring multifaceted immune reactions to vaccines.[29,30] In contrast to PEI, CpG ODNs trigger the TLR-9 innate signaling pathway, programming Th1-biased responses.[31] The incorporation of CpG and antigens into the same nanoparticle enhanced cellular immune responses.[32,33] Here we prepared uniform and spherical PEI-HA and PEI-HA/CpG nanoparticles and then evaluated their immunogenicity by a prime-boost i.n. vaccination strategy in mice.

Our results revealed that intranasal immunization with the resulting nanoparticle vaccines significantly enhanced the immunogenicity of influenza HA proteins and induced heterologous influenza immunity (Figure 1A). Notably, the nanoparticle immunization generated strong antibody responses to the conserved HA stalk. PEI-HA nanoparticles generated Th2-biased IgG1-dominant antibody response and faint cellular response. By contrast, PEI-HA/CpG nanoparticles generated a robust and comprehensive immunity, including balanced IgG1/IgG2a antibody responses with augmented neutralizing antibody titers, Fc-mediated ADCC responses, and IFN-γ-mediated cellular immune responses. The PEI-HA/CpG nanoparticle-induced immune responses were long-lasting, providing improved cross-protection efficacy compared to PEI-HA against heterologous viral challenges six months postimmunization, with significantly diminished body-weight loss and pulmonary immunopathology in mice. The complementary and synergistic adjuvant effects of PEI and CpG account for the boosted HA-induced cross-protective influenza immunity.

RESULTS

Fabrication and Characterization of PEI Nanoparticles. We produced recombinant trimeric A/Aichi/2/1968 (H3N2) HA (designated as H3) and determined the antigenicity and purity of the obtained H3 in our previous study.[34] PEI-H3 and PEI-H3/CpG nanoparticles were prepared by a simple electrostatic assembly method (Figure 1A). The negatively charged proteins and CpG can

https://doi.org/10.1021/acsami.1c19192
ACS Appl. Mater. Interfaces 2022, 14, 6331−6342

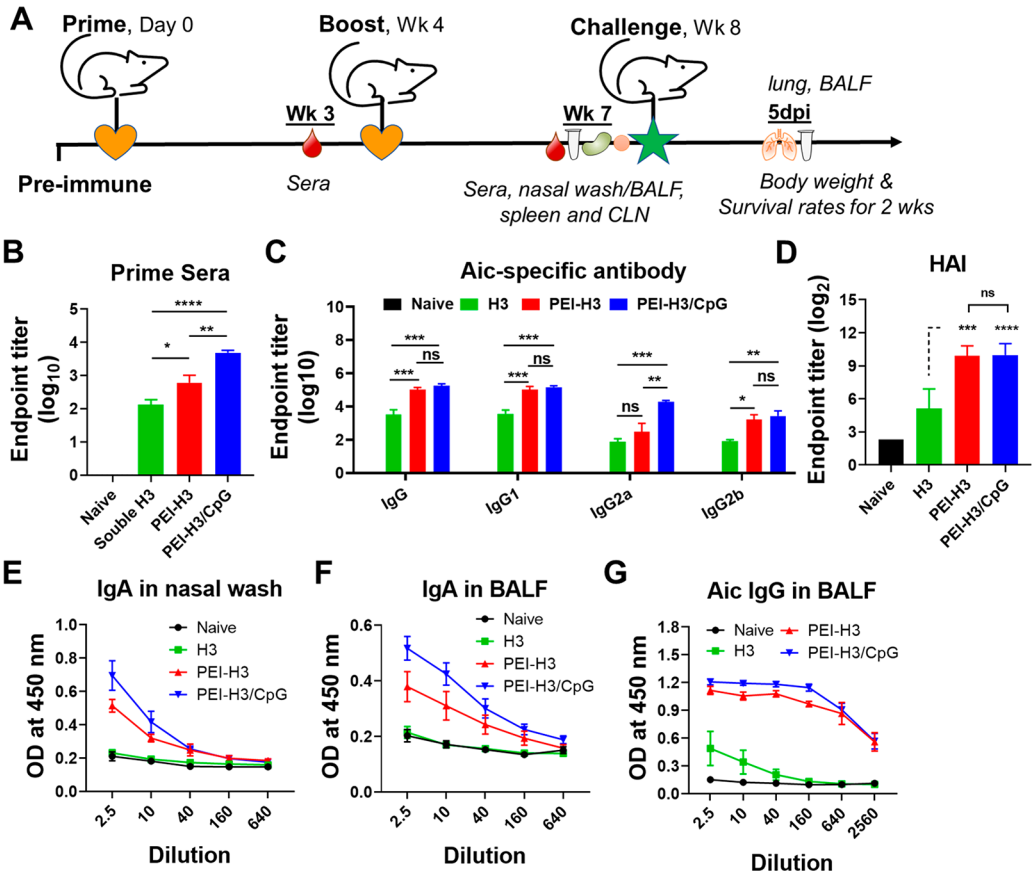

Figure 2. Antibody responses. (A) Immunization, challenges, and sampling schedule. (B) Aichi-specific IgG levels in prime sera. (C) Aichi-specific IgG and IgG subtype levels in boost sera. (D) HAI titers in boost sera. (E−G) Aichi-specific antibody levels in mucosal washes. Data are presented as mean ± SEM (n = 5 for B−D, n = 3−4 for E−G). One-way ANOVA then Tukey's multiple comparison tests were used for statistical significance analysis (*p < 0.05; **p < 0.01; ***p < 0.001; ****p < 0.0001; ns, p > 0.05).

spontaneously complex with PEI to form uniform nanoparticles via electrostatic interactions.

To optimize the PEI-H3 nanoparticle size for intranasal immunization, we prepared the nanoparticles with different PEI/H3 ratios (2:1, 1:1, 1:2, and 1:4). We achieved the best nanoparticle size distribution (PDI index of 0.113) at a ratio of 2:1 (Figure 1B and 1C) as determined by dynamic light scattering (DLS) and transmission electron microscopy (TEM). The nanoparticles were relatively uniform nanospheres of around 100 nm in diameter. We used the ratio of 2:1 in subsequent studies, as relatively smaller particle sizes are favorable for transmucosal delivery through M cells and lymph node trafficking of particulate vaccines.[35]

We prepared PEI-H3/CpG nanoparticles by coloading H3 with CpG. The branched PEI completely absorbed CpG molecules (Figure 1D). Strong H3 signals were observed from soluble H3, PEI-H3, and PEI-H3/CpG nanoparticle solutions on the Coomassie-blue-stained SDS-PAGE (Figure 1E). The resulting PEI-H3/CpG nanoparticles were around 120 nm (Figure 1C) and exhibited positive surface charges (Figure S1A). Additionally, the nanoparticle size was stable at 4 °C for at least four months (Figure S1B).

Induction of Humoral and Cellular Immune Responses. We performed a simple safety study of the PEI-H3 nanoparticles postvaccination. We did not observe significant body weight changes or inflammation in lung tissues 7 days postvaccination (Figure S2). Another study has previously indicated that an intranasal administration of 20 μg of PEI did not significantly affect murine nasal epithelium compared with PBS alone.[26]

We used a two-dose intranasal vaccination program to study the immunogenicity of the PEI nanoparticles (Figure 2A). We titrated the serum antibodies to the Aichi virus (Figure 2B and 2C) and found that the nanoparticles induced significantly higher IgG titers than soluble H3. The PEI-H3/CpG generated significantly higher IgG levels than PEI-H3 in prime sera (Figure 2B). Despite the comparable IgG, IgG1, and IgG2b levels, the PEI-H3/CpG group had significantly higher IgG2a titers in the boost sera than PEI-H3 (Figure 2C). We also observed similar results in the induction of serum H3-specific antibody levels (Figure S3). Overall, PEI-H3 nanoparticles generated a potent IgG1-dominant antibody response. By contrast, the PEI-H3/CpG nanoparticles induced comprehensive, diverse, and more balanced IgG1/IgG2a antibody responses. Furthermore, the nanoparticles induced significantly higher Aichi virus-specific hemagglutination−inhibition (HAI) titers than the soluble H3 group (Figure 2D). There was no statistical difference in HAI between the two nanoparticle groups.

We further investigated the mucosal antibody responses 3 weeks postboosting immunization. We detected little sIgA in nasal washes and BALF from the soluble H3 group (Figure 2E and 2F). In contrast, the nanoparticles generated significantly higher IgA antibody levels than the naïve and soluble H3 groups. The PEI-H3/CpG induced higher IgA levels than PEI-H3 in nasal washes and BALF. Compared with the low IgG

https://doi.org/10.1021/acsami.1c19192
ACS Appl. Mater. Interfaces 2022, 14, 6331−6342

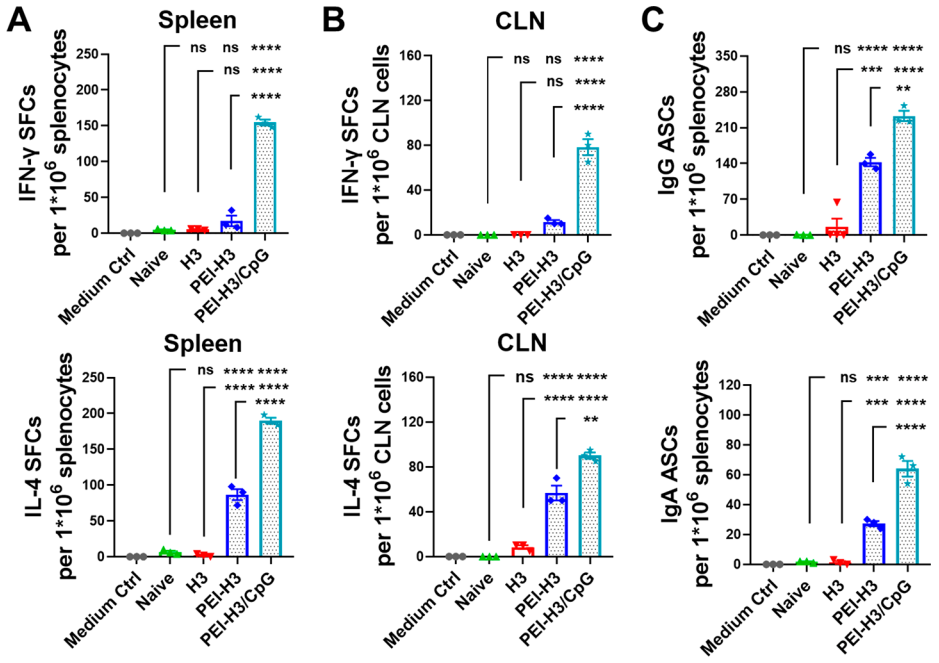

Figure 3. Cellular immune responses. (A,B) H3-specific IFN-γ and IL-4-producing spot-forming-cell (SFC) populations. (C) H3-specific antibody-secreting cells (ASCs) postimmunization. Data are presented as mean ± SEM (n = 3). One-way ANOVA then Tukey's multiple comparison tests were used for statistical significance analysis (*p < 0.05; **p < 0.01; ***p < 0.001; ****p < 0.0001; ns, p > 0.05).

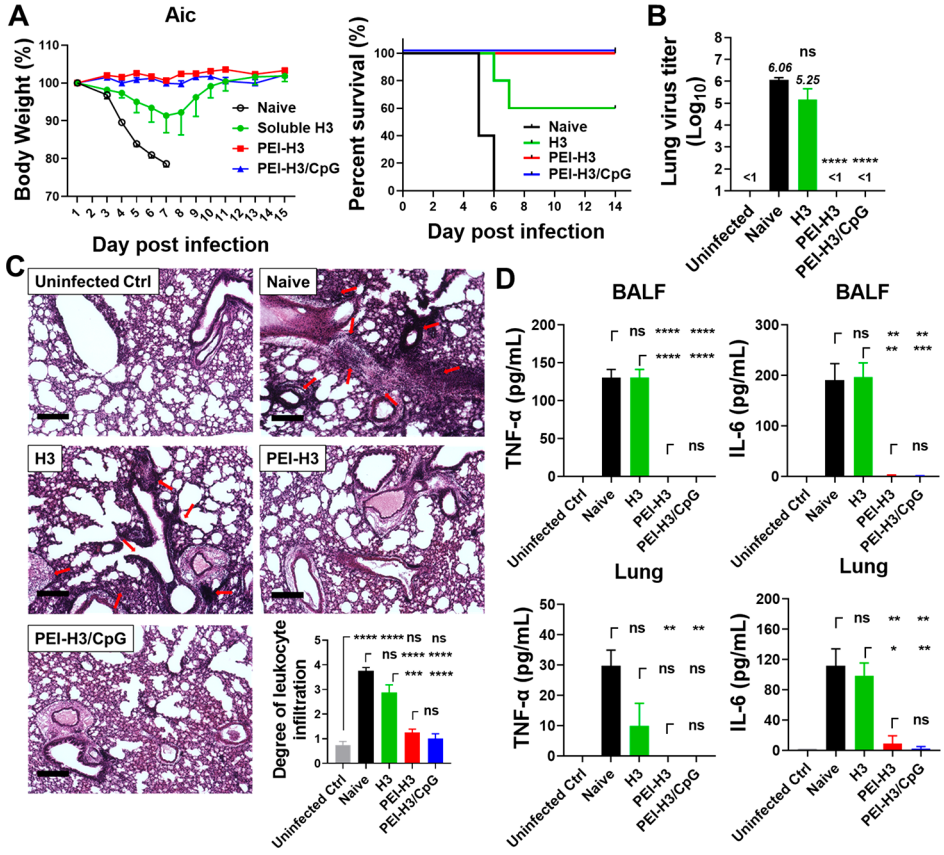

Figure 4. Homologous influenza virus challenge. Mice were challenged with 15 × LD_{50} of mouse-adapted Aichi (Aic) viruses 4 weeks postimmunization. (A) Mouse morbidity and mortality. (B) Lung virus titers. (C) Histological pathology analysis. Red arrows indicate leukocyte infiltration. Bars represent 200 μm in length. The bar chart shows the leukocyte infiltration scores. (D) TNF-α and IL-6 levels in BALF. Data are presented as mean ± SEM (n = 3 for A and n = 3−4 for B−D). Statistical significance was analyzed by a one-way ANOVA and Tukey's multiple comparison tests (*p < 0.05; **p < 0.01; ***p < 0.001; ****p < 0.0001; ns, p > 0.05).

https://doi.org/10.1021/acsami.1c19192
ACS Appl. Mater. Interfaces 2022, 14, 6331−6342

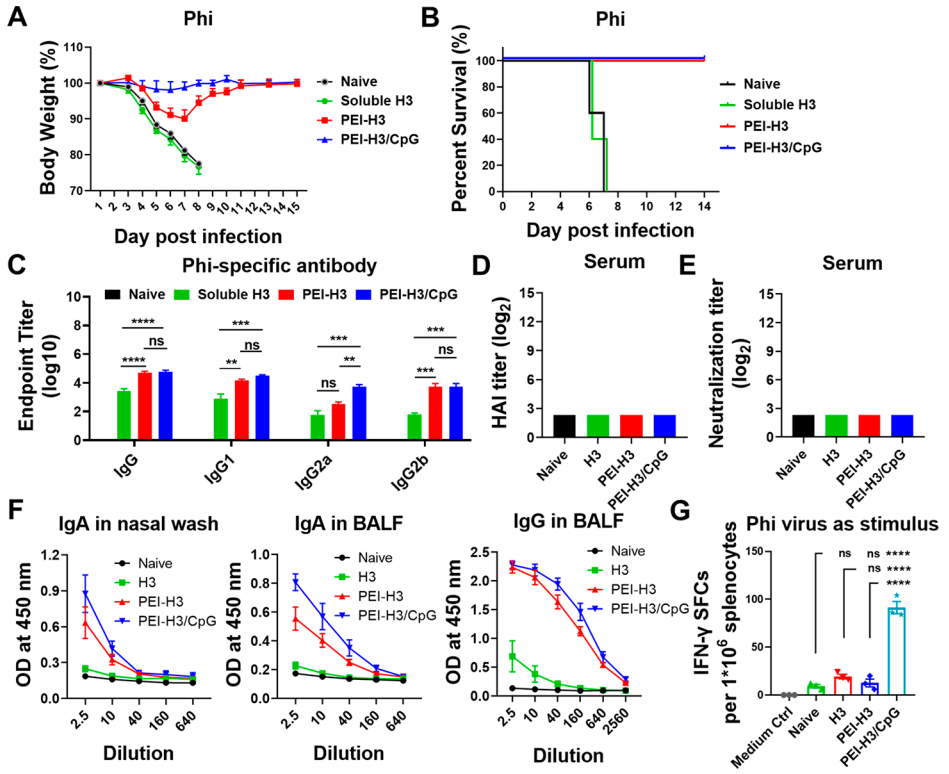

Figure 5. Heterologous virus challenge. Mice were challenged with 2 × LD_{50} of mouse-adapted Philippines (Phi) viruses 4 weeks postimmunization. (A, B) Morbidity and mortality. (C) Phi virus-specific antibody levels in immune sera. (D, E) HAI titers and neutralizing antibody titers. (F) Antibody levels in nasal washes and BALF. (G) Phi-specific IFN-γ-secreting splenocytes. Data are presented as mean ± SEM (n = 5 for A−E and n = 3−4 for F,G). One-way ANOVA then Tukey's multiple comparison tests were employed for statistical significance analysis (*p < 0.05; **p < 0.01; ***p < 0.001; ****p < 0.0001; ns, p > 0.05).

levels in the H3 group, the nanoparticles caused significantly higher IgG levels in BALF (Figures 2G). Therefore, intranasal immunization with these PEI nanoparticles significantly boosted both local and systemic antibody responses in mice.

We determined the antigen-specific IFN-γ- and IL-4-secreting cell frequencies in immunized mouse spleens. The soluble H3 generated few IFN-γ- or IL-4-secreting splenocytes 3 weeks after the second vaccination (Figure 3A). The PEI-H3 nanoparticle potently boosted the generation of IL-4-secreting cells, suggesting Th2-biased immune responses. By contrast, PEI-H3/CpG nanoparticles boosted both IL-4- and IFN-γ-secreting splenocytes. In addition, we observed similar results from the draining cervical lymph node (CLN) lymphocytes (Figure 3B).

At 3 weeks postimmunization, we consistently detected elevated amounts of antigen-specific IgG and IgA ASCs in the nanoparticle groups but not the H3 group (Figure 3C). In addition, we observed significantly higher IL-4-secreting splenocytes and antibody-specific IgG and IgA ASCs in the PEI-H3/CpG group versus the PEI-H3 group. The ASC frequency also correlates well with the antibody levels. Therefore, PEI-H3/CpG nanoparticle vaccination significantly boosted Th1 and Th2 immune responses and correlated plasma B cell generation.

Protective Efficacy against Homologous Influenza Infection. We investigated the protective efficacy of the nanoparticle vaccine immunization against the homologous virus challenged with the 15 × LD_{50} mouse-adapted Aichi virus (Figure 4). All the naïve mice rapidly deteriorated and died in days 7 to 8 (Figure 4A). We observed diminished weight loss (compared with naïve mice) and partial protection (60% survival rate) in the soluble H3 group. In contrast, the nanoparticle groups had a 100% survival rate without apparent bodyweight loss.

The lung virus titers were analyzed 5 days postchallenge. Naïve and soluble H3-immunized mice showed high lung virus titers of 1 × $10^{6.06}$ $TCID_{50}$ and 1 × $10^{5.25}$ $TCID_{50}$, respectively (Figure 4B). In comparison, the nanoparticle groups displayed undetectable lung virus titers.

We studied pulmonary immunopathology by performing histological examinations of the mouse lungs with H&E staining. Naïve mice developed a severe inflammatory state with massive leukocyte infiltration in the lungs. Soluble H3 immunization decreased the inflammation but with noticeable leukocyte infiltration. In contrast, the nanoparticles-immunized mice showed significantly reduced inflammation and leukocyte infiltration (Figure 4C). Additionally, the nanoparticle groups displayed significantly decreased inflammatory cytokine levels (TNF-α and IL-6) in mouse BALF and lung homogenate (Figure 4D).

Therefore, PEI nanoparticle i.n. vaccination induced comprehensive immune protection against homologous virus infection in mice, manifested by decreasing lung virus replication, inflammation, and leukocyte infiltration.

Protective Efficacy against Heterologous Influenza Infection. We applied A/Philippines/2/1982 (Phi, H3N2) in the heterologous challenge study to investigate the cross protection in vaccinated mice. As shown in Figures 5A and 5B, all mice that did not receive nanoparticle immunizations quickly lost weight and perished a week postinfection. By

https://doi.org/10.1021/acsami.1c19192
ACS Appl. Mater. Interfaces 2022, 14, 6331−6342

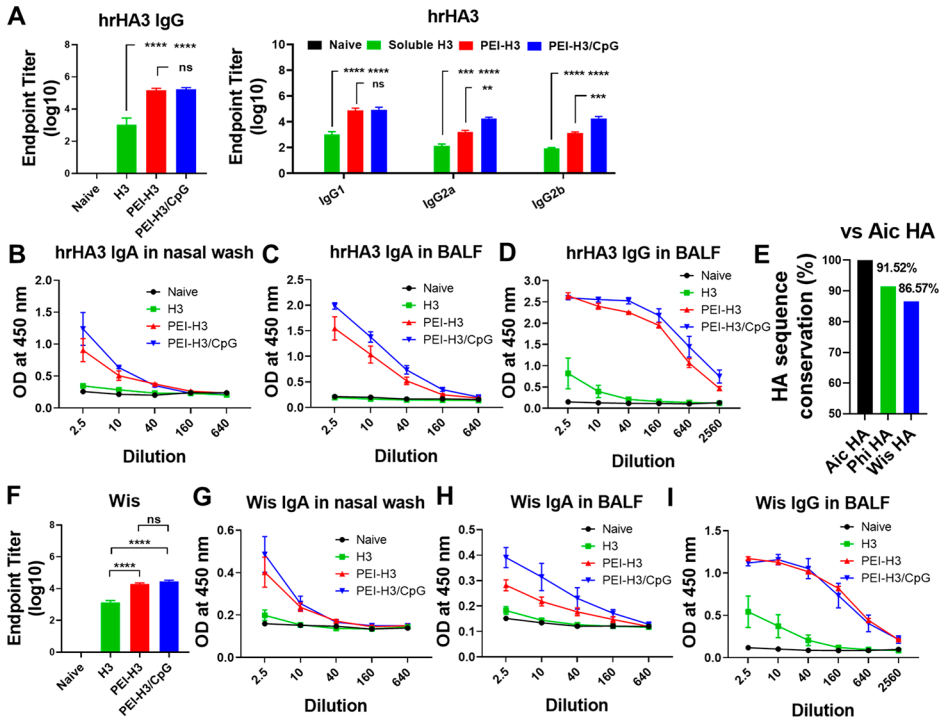

Figure 6. Cross-reactive antibody responses. (A) Serum hrHA3-specific IgG, IgG1, IgG2a, and IgG2b levels in mouse sera. (B–D) hrHA3-specific antibody levels in mucosal washes. (E) HA sequence conservation ratio vs Aic HA. (F–I) Wis virus-specific antibody levels in mouse sera and mucosal washes. Data are presented as mean ± SEM (n = 5 for A and F and n = 3–4 for B–D and G–I). One-way ANOVA then Tukey's multiple comparison tests were utilized for statistical significance analysis (*p < 0.05; **p < 0.01; ***p < 0.001; ****p < 0.0001; ns, p > 0.05).

contrast, the PEI-H3 and PEI-H3/CpG nanoparticles protected all the vaccinated mice with 100% mouse survival rates. Furthermore, compared with PEI-H3-immunized mice that suffered apparent bodyweight loss postinfection, PEI-H3/CpG-immunized mice were protected against body weight loss.

Consistent with the challenge results, we detected cross-reactive Phi-specific IgG, IgG1, IgG2a, and IgG2b levels in the immune sera of nanoparticle-vaccinated mice (Figure 5C). However, no apparent HAI and neutralization activities against Phi were detected (Figure 5D and 5E). In nanoparticle-vaccinated mice, we also saw significantly elevated cross-reactive mucosal antibodies, including sIgA in nasal washes and sIgA and IgG in BALF (Figure 5F). The PEI-H3/CpG nanoparticles induced the greatest antibody titers in sera and mucosal washes, with a significantly higher serum IgG2a antibody level than the PEI-H3 nanoparticles.

In addition to the cross-reactive antibody responses, cellular responses may also protect against heterologous challenges. We determined the IFN-γ-secreting splenocytes by Elispot assay. Under stimulation with the Phi virus, the PEI-H3/CpG group, but not the soluble H3 or PEI-H3 group, displayed substantial IFN-γ-secreting splenocyte populations (Figure 5G).

Therefore, PEI-H3/CpG nanoparticles demonstrated the best cross-protection efficacy against heterologous virus infection in mice. The cross-reactive antibody responses and the IFN-γ-mediated protective cellular immune responses are essential components of the protective scenario, protecting the mice against bodyweight loss postinfection.

Cross-Reactive Antibody Responses. We detected the antibody levels against the head-removed, more conserved Aichi HA stalk (hrHA3). We observed elevated hrHA3-bound antibody titers in the immune sera of the PEI-H3 and PEI-H3/CpG nanoparticle groups (Figure 6A). Despite the comparable serum IgG and IgG1 levels, PEI-H3/CpG induced significantly higher hrHA3-specific IgG2a and IgG2b titers than PEI-H3. The nanoparticle groups also boosted the hrHA3-specific IgA and IgG production in mouse nasal washes and BALF (Figure 6B–6D).

As hrHA3-specific IgG2a and IgG2b are highly efficient in inducing Fc-mediated functions such as ADCC,[36] we performed an ADCC surrogate assay with mouse immune sera at 1:250 dilution. The PEI-H3/CpG group showed significantly higher serum ADCC activity than the H3 and PEI-H3 groups (Figure S4).

We also studied the antibody cross reactivity against the A/Wisconsin/15/2009 (Wis, H3N2) strain. A comparison of Aic and Wis HA amino acid sequences showed a difference of 13.43%, which was higher than that (8.48%) between Aic and Phi (Figure 6E and Table S1). Despite the substantial antigenic drift, the nanoparticles induced significantly higher serum IgG levels specific to Wis than soluble H3 (Figure 6F). We also observed significantly elevated cross-reactive sIgA in nasal washes and higher sIgA and IgG in BALF of the nanoparticle groups (Figure 6G–6I).

Immune Duration and Protection Efficacy. We studied the long-term antibody responses against the conserved hrHA3, Phi, and Aic viruses over six months postboosting immunization. Here we included the soluble H3+CpG group for comparison. Our results showed that the nanoparticle vaccines induced more durable and long-lasting antibody responses that did not decay over six months postimmunization, particularly against the conserved hrHA3 (Figure 7A and Figure S5). By contrast, antibodies in the H3- and H3+CpG-immunized mice gradually decreased.

https://doi.org/10.1021/acsami.1c19192
ACS Appl. Mater. Interfaces 2022, 14, 6331–6342

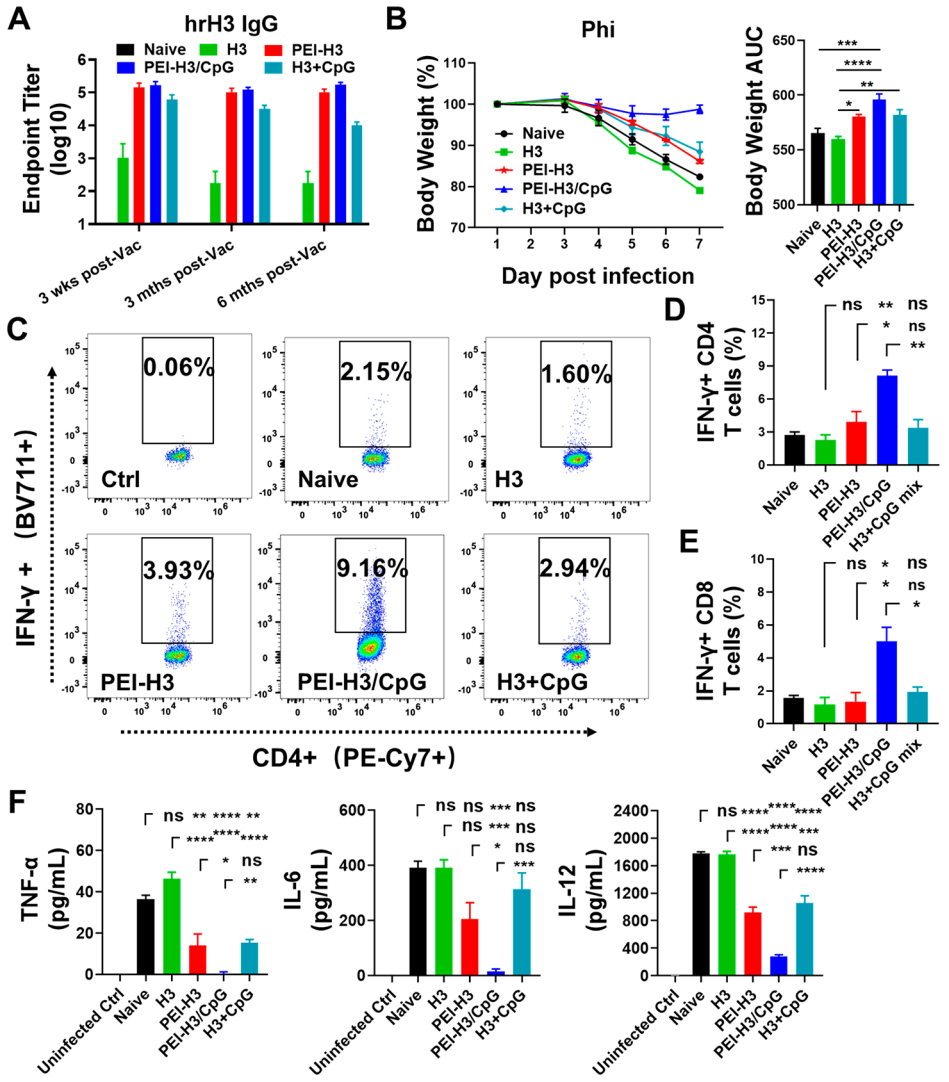

Figure 7. Immune duration and protection against the Phi challenge. (A) Serum hrHA3-specific IgG antibody titers at different time points. Wks, weeks. Mths, months. Vac, vaccination. (B) Mice body weight changes and area under the curve (AUC) in 6 days postchallenge with Phi. (C–E). IFN-γ-secreting CD4+ and CD8+ T lymphocytes in mouse BALF. (F) BALF TNF-α, IL-6, and IL-12 levels. Data are presented as mean ± SEM (n = 5 for A, n = 3–4 for B–E). One-way ANOVA then Tukey's multiple comparison tests were employed for statistical significance analysis (*p < 0.05; **p < 0.01; ***p < 0.001; ****p < 0.0001; ns, p > 0.05).

We studied the long-term protective efficiency against the Phi challenge. The nanoparticle vaccines showed superior protection in mice to H3 alone. Mice in the PEI-H3/CpG nanoparticle group displayed the least bodyweight loss (Figure 7B). By contrast, the mice in the PEI-H3 and H3+CpG groups suffered dramatic weight loss. Consistently, we detected significantly boosted IFN-γ-secreting CD4+ and CD8+ T lymphocytes in the PEI-H3/CpG nanoparticle group than any other group (Figure 7C–7E).

We studied the pulmonary immunopathology by detecting the inflammatory cytokine (TNF-α, IL-6, and IL-12) levels in mouse BALF postchallenge (Figure 7F). The PEI-H3 and H3+CpG groups displayed decreased inflammatory cytokine levels compared to naïve and soluble H3 groups. The PEI-H3/CpG nanoparticle-immunized mice displayed the lowest inflammatory cytokine levels among all groups. We also detected the lowest inflammatory cytokine levels in lung homogenate of infected mice (Figure S6).

DISCUSSION

Vaccination represents a cost-effective strategy to combat influenza infection. Intranasal vaccination with recombinant proteins is an excellent developmental model for cross-protective influenza vaccines in terms of good safety, rapid and scalable manufacturing, and multifaceted protective immune responses. However, the low immunogenicity of intranasally administered recombinant proteins has hindered their application as intranasal vaccines and necessitates the development of mucosal adjuvants.

Adjuvants (adjuvanted nanoparticles or molecular adjuvants) boost the immune responses of intranasal vaccines via different mechanisms. No single adjuvant, however, can produce the optimal innate notch nursing the adaptive immune responses required for broad influenza immunity. Proper adjuvant combinations may work complementarily and synergistically to induce the necessary multifaceted immune responses against both homologous and variant strains. Nanoparticle adjuvant systems have demonstrated superior advantages in developing intranasal vaccines.[2,37] Previously, we

https://doi.org/10.1021/acsami.1c19192
ACS Appl. Mater. Interfaces 2022, 14, 6331–6342

reported that a PEI-functionalized graphene oxide (GO) nanoparticle vaccine platform significantly enhanced the antigen immunogenicity. However, the probable long-term retention of the inorganic GO materials raises major safety concerns.

Here, we prepared protein nanoparticles directly with PEI. This method was protein friendly, did not require chemical cross-linkers or organic solvents, and was easily adapted for various vaccine components. A previous study indicated that PEI targeted epithelial cells and microfold cells (M cells) and promoted transmucosal antigen delivery to dendritic cells in cervical lymph nodes (CLNs) in an intranasal route.[26] PEI also modestly and transiently recruited neutrophils into the nasal-associated lymphoid tissue (NALT) and CLNs and significantly recruited dendritic and B cells to CLNs. Moreover, we found that the PEI nanoparticle adjuvant system displayed a superior synergistic boosting effect when cooperated with molecular adjuvant CpG for protein antigens in this study. The coencapsulated CpG in the nanoparticles significantly improved PEI-adjuvanted vaccines' poor/faint Th1 cellular responses. The PEI-HA/CpG nanoparticles possessed multiple features favorable for enhancing antigen immunogenicity, including a uniform size distribution that resembled viruses in size, long-term stability, enhanced transmucosal delivery, and synergistic adjuvant effects. The PEI-HA/CpG nanoparticles induced a more comprehensive immune response versus soluble HA and PEI-HA nanoparticles with multifaceted immunoenhancing features.

HA is the immunodominant surface protein of influenza viruses. Antibody responses are the essential effector function in influenza HA-mediated influenza protection. Vaccine-induced IgG isotypes (IgG1 and IgG2a) play divergent but important roles in stemming influenza infection.[38,39] IgG1 is associated with virus neutralization, preventing virus attachment to target cells. In contrast, IgG2a activates Fc receptor-mediated effector responses and correlates with the clearance of the virus from infected hosts. In our study, soluble H3 showed poor immunogenicity, as indicated by the low antibody levels postvaccination. Soluble HA provided partial protection against the homologous Aic virus challenge but no protection against heterologous Phi. The PEI-HA nanoparticles significantly boosted antibody production and significantly improved the protection against both Aic and Phi challenges despite apparent bodyweight loss post the Phi challenge. In addition, PEI-HA boosted Th2-biased IgG1 subtype production, consistent with a previous report.[26] In comparison, PEI-HA/CpG nanoparticles containing small amounts (1 ug) of CpG had a potentiating effect on the Th1-type antibody response and induced more balanced IgG1 and IgG2a antibody responses.

Boosted neutralizing antibodies are the main contributors for protection against homologous or close virus strains but not against distantly related strains. Compared with IgG1, murine IgG2a and IgG2b can more efficiently activate the cell-mediated immune response, such as complementary and antibody-dependent cytotoxic response.[40,41] Our study detected no cross-neutralizing antibodies against the Phi virus due to the Phi's genetic distance from the vaccine strain. The boosted protective IgG2a-mediated effector responses, including ADCC function, contributed to the improved heterologous protection in the PEI-H3/CpG group versus the PEI-H3 group. The PEI-H3/CpG nanoparticle significantly boosted diversified antibodies, resulting in superior protection against homologous and heterologous viruses.

Influenza HA has a head and a stalk region. Current influenza vaccines elicit immune responses against the immunodominant and variable globular HA head. Most neutralizing antibodies recognize the HA head domain.[40] However, the HA head domain is highly mutable, accounting for the lowered efficiency against mismatched strains. In comparison, the HA stalk domain has a higher degree of conservation. In our study, the nanoparticle immunization strongly enhanced the production of hrHA3-specific antibodies in an IgG1/IgG2a mixed fashion. HA stalk-binding antibodies are valued in vaccine research as potent inducers of ADCC for optimal protection in vivo.[42] Moreover, our studies indicated that the nanoparticles induced long-lasting and durable hrHA3-specific immune responses, as shown by the sustained high antibody levels.

Cellular immunity plays a significant role in clearing infected cells and is the major mediator of cross-protection against variant strains when neutralizing antibodies are absent.[43−45] In our study, substantial IFN-γ-secreting splenocytes were observed only in the PEI-H3/CpG nanoparticle group. In addition to promoting B-cell differentiation in a Th1-biased mode—thus facilitating Fc-mediated effector functions in mice—IFN-γ plays important protective roles in activating macrophages and NK cells, inducing phagocytosis, promoting up-regulation of major histocompatibility complex (MHC) class I presentation, and activation of CD8+ T cell responses.[45] CD8+ T cells can promote efficient virus elimination and quick host recovery following distinct influenza virus strain challenges.[46] Multifunctional CD4 effector cells expressing IFN-γ and perforin were reported to have cytolytic activity and mediate protection recovery from influenza virus infection.[47] We also detected IFN-γ-secreting CD4+ and CD8+ T cell responses in mouse BALF and the associated cross-protection against a heterologous Phi challenge after six months postboosting immunization, indicating the importance of local mucosal protective cellular immunity. The IFN-γ-mediated cellular immune responses in systematic and local sites and the improved antibody responses together contributed to the enhanced cross protection of PEI-H3/CpG nanoparticles against the heterologous virus challenge.

As a cationic polymer abundant in amine groups, PEI can deliver protein antigens to the cytoplasm via an endosome-disruptive effect, which is critical in cross-presenting exogenous antigens to induce CD8+ T cell responses.[48] However, CD8+ T cell responses in the PEI-H3 group were muted by a lack of IFN-γ secretion, consistent with the previous report with gp140.[26] By contrast, the PEI-H3/CpG group generated improved protection against Phi virus infection via protective cellular responses. PEI-H3/CpG was a more potent inducer of cellular immune responses than PEI-H3 due to Th1 responses and IFN-γ induced by the coloaded CpG. Moreover, the nanoparticle formulation enhanced the CpG adjuvant effect as indicated by the superior protection and boosted IFN-γ-secreting T lymphocytes in the PEI-H3/CpG vs H3+CpG group.

Therefore, the combination of PEI and CpG in the PEI-H3/CpG nanoparticle group contributed to the multifaceted immune responses, leading to robust cross protection against influenza. The PEI-H3/CpG nanoparticles show good potential as a cross-protective influenza vaccine candidate. However, despite no apparent adverse effects observed in our

https://doi.org/10.1021/acsami.1c19192
ACS Appl. Mater. Interfaces 2022, 14, 6331−6342

study, a more comprehensive safety evaluation of this nanoparticulate adjuvant system is needed before clinical trials.[49,50] In addition, systematic optimization of this system, including the molecular structure (branched or linear) and molecular weight of PEI, would further benefit such mucosal vaccine development.

CONCLUSIONS

In summary, PEI served as a robust and versatile delivery system to simultaneously carry antigens (HA) and adjuvants (CpG) for optimal immunoenhancement. The PEI nanoparticle vaccines potently enhanced the immunogenicity of intranasally administered influenza HA and generated substantial antibodies against the conserved stalk region of HA. Compared with PEI-H3, PEI-H3/CpG nanoparticles demonstrated multifaceted immune responses, including robust, balanced Th1/Th2 antibody responses and potent cellular responses with abundant IFN-γ induction, resulting in improved cross protection against influenza. PEI and CpG synergized this cross-protective influenza immunity. We also observed that these comprehensive immune responses and cross protection were long lasting over six months post-immunization. Therefore, PEI-H3/CpG nanoparticles have the potential as a cross-protective influenza vaccine candidate. Polycationic PEI nanoplatforms merit future development as potent mucosal delivery systems.

MATERIALS AND METHODS

Ethics Statement and Statistical Analysis. Animal studies were carried out in strict compliance with the Institutional Animal Care and Use Committee (IACUC) guidelines of Georgia State University under protocol A19025. Means and the standard errors of the mean (SEM) were employed for data presentation. Statistical significance between groups was analyzed by the one-way analysis of variance (ANOVA) using GraphPad Prism 8 (GraphPad software). A p-value <0.05 is recognized as statistically significant, and $p < 0.01$ or $p < 0.001$ was considered extremely significant: $P > 0.05$ (ns), $p < 0.05$ (*), $p < 0.01$ (**), $p < 0.001$ (***), and $p < 0.0001$ (****).

Materials, Cell Lines, and Viruses. Branched PEI was ordered from Sigma-Aldrich. CpG ODN1826 was a product of InvivoGen, USA. *Spodoptera frugiperda* (Sf9, ATCC, CRL-1711) insect cells were cultured in protein-free ESF 921 (Expression Systems, USA). Aichi HA (H3) and hrHA3 were expressed and purified as described previously.[34] Purified proteins were assayed using a BCA assay kit (Thermo Fisher Scientific, USA).

Madin-Darby canine kidney (MDCK, ATCC CCL-34) cells were grown in Eagle's Minimum Essential Medium (EMEM, ATCC 30−2003) supplemented with 10% heat-inactivated fetal calf serum (FCS, ATCC 30−2020) and 1% penicillin/streptomycin in a CO_2 (5%) incubator at 37 °C. HEK 293T (ATCC CRL-3216) cells were grown in Dulbecco's Modified Eagle's Medium (DMEM) (ATCC 30−2002) containing 10% FCS and 2 mM L-glutamine (ATCC 30−2214).

Influenza A/Aichi/2/1968 (Aic, H3N2) and A/Philippines/2/1982 (Phi, H3N2) were passaged in embryonated chicken eggs. Mouse-adapted Aic and Phi were expanded in intranasally (i.n.) infected mouse lungs. The standard Reed and Muench method was used to measure the virus median lethal dose (LD_{50}).

Fabrication of PEI-H3 and PEI-H3/CpG Nanoparticles. For PEI-H3 and PEI-H3/CpG nanoparticle fabrication, equal volumes of PEI and H3 or H3/CpG solutions in sterile PBS were mixed for 1 min. PEI-H3 nanoparticles were generated at PEI/H3 ratios of 2:1, 1:1, 1:2, or 1:4 to determine the influence of feeding ratios on the size and size distribution of resulting nanoparticles. The particle size and zeta potentials were characterized using dynamic light scattering (DLS, Malvern 10 Zetasizer Nano ZS, Malvern Instruments, USA). The nanoparticle morphology was characterized by transmission electron microscopy (TEM, Jeol JEM-100CX II at 100 kV) after negative staining with 1% phosphotungstic acid (PTA, pH 7.4) for 1 min.

The H3 in PEI-H3 and PEI-H3/CpG nanoparticles was characterized by reducing SDS-PAGE followed by Coomassie Blue (Bio-Rad, USA) staining. The gel images were captured with the ChemiDoc Touch imaging system (Bio-Rad). Agarose gel electrophoresis was used to study free CpG molecules in the PEI-H3/CpG formulation solutions. Briefly, the PEI-HA/CpG nanoparticle suspension and soluble free CpG solution containing an equal amount of CpG molecules were analyzed by electrophoresis (1% agarose gel, 30 kV for 10 min).

Immunization Studies. BALB/c mice (six- to eight-week-old, female) were intranasally (i.n.) immunized with different vaccine formulations in 25 μL of saline. Mouse body weight changes were recorded for 7 days postvaccination, and lung histological studies by H&E staining were performed after that to evaluate the in vivo safety of the PEI-H3 nanoparticles in mice.

To study the induction of immune responses, mice were vaccinated twice with soluble H3, PEI-H3, or PEI-H3/CpG nanoparticles containing 5 μg of H3 at an interval of 4 weeks. Prime and boost sera ($n = 5$) were collected 3 weeks postpriming immunization and boosting immunization, respectively.

At 3 weeks postboosting immunization, immunized mice ($n = 3$−4) were sacrificed to collect nasal washes and bronchoalveolar lavage fluid (BALF) by flushing the respective cavities with 1 mL of cold, sterile PBS with 5% BSA. Cervical lymph nodes (CLNs) and spleens were also isolated to prepare single-cell suspensions.

To study the immune protection efficacy, mice ($n = 5$) were intranasally challenged with 15 × LD_{50} of mouse-adapted Aic or 2 × LD_{50} of Phi in 25 μL of cold saline 4 weeks postboosting immunization. We monitored mouse body weight changes daily for 2 weeks postchallenge. A weight drop >20% was used as a humane end point.

Humoral and Cellular Immune Response Assays. Virus-specific antibody titers in immune sera, nasal washes, and BALF postimmunization were evaluated as described previously.[51] Hemagglutination-inhibition (HAI) assays were performed as reported.[24]

For the microneutralization (MN) assay, viruses were titrated after 18 h coincubation with MDCK cells by an ELISA assay detecting the influenza virus nucleoprotein following a WHO-recommended protocol. The Reed−Muench method was employed to calculate the median tissue culture infective dose ($TCID_{50}$) titer. Serial dilutions of heat-inactivated (56 °C, 30 min) immune sera were mixed with 100-fold $TCID_{50}$ of virus for 2 h at 37 °C. Then the mixture was incubated with precoated MDCK cell monolayers (1.5×10^4 cells/well) for 18 h in the presence of 2 μg/mL of TBCK trypsin. The virus inhibition was determined as previously described.[52]

The ELISpot assay was employed to evaluate the numbers of IL-4 or IFN-γ-secreting cells and antibody (IgG and IgA)-secreting cells (ASCs) in mouse spleens and cervical lymph nodes 3 weeks after boosting immunization, as described previously.[19]

The ADCC surrogate assay was carried out for mouse immune sera at 1:250 dilution according to the ADCC reporter bioassay kit protocol (Promega, Cat No. M1211) with modification. pCAGGS plasmids encoding H3-transfected HEK-293T cells and mFcγRIV-expressing Jurkat cells in the kit were used as target and effector cells, respectively. After incubation for 6 h, a Bio-Glo Luciferase substrate was added, and the luminescence intensity was recorded as luminescence relative light units (RLUs) by a GloMax (Promega).

Histological Examination, Virus Titration, and Inflammatory Cytokine Evaluation. Mice ($n = 3$−4) were sacrificed 5 days postinfection with 15 × LD_{50} of Aichi virus. Mouse lungs were isolated for histological examination and lung viral titers determination as previously described.[19] Histological analysis was performed by Hemotoxylin and Eosin (H&E) staining of the paraffin-embedded lung sections. The stained sections were imaged with a Keyence BZ-X710 microscope. The leukocyte infiltration degree was scored.

Lung tissues were ground on a 70 μm Nylon cell strainer (Falcon) to collect the supernatants for lung viral titer determination.

https://doi.org/10.1021/acsami.1c19192
ACS Appl. Mater. Interfaces 2022, 14, 6331−6342

Quadruplicate 10-fold serial dilutions (100 μL) were cocultured with MDCK cells (1.5×10^5 cells/mL, 100 μL) for 4 days in 96-well plates. A standard hemagglutination assay was used to calculate the hemagglutinin activity titers. The Reed−Munches method was employed to determine the lung viral titers. TNF-α and IL-6 levels in the BALF were determined using the cytokine assay kits (Thermo Scientific).

Long-Term Immune Studies. To study the long-term immune responses, we evaluated the Aic virus and hrHA3-specific antibody levels at 3- and 6-months postboosting immunization and then challenged the mice (n = 3−4) with 2 × LD_{50} of the Philippines virus. Here we included the H3+CpG group. After monitoring the mouse body weight changes daily for 6 days, we euthanized the mice, collected the mucosal BALF lymphocytes, and studied the local cellular responses by flow cytometry.[53] Briefly, after antigen restimulation for 5 h in the presence of a Golgi stopper (BD Biosciences, 2 μg mL^{-1}), the cells were stained by CD4-PE-Cy7 and CD8-PE-Cy5 antibodies (BD Biosciences). After fixation and permeabilization, intracellular staining with IFN-γ-BV711 (BioLegend) was performed. IFN-γ-secreting T lymphocytes were recorded by flow cytometry (BD LSRFortessa) and analyzed by FlowJo software.

■ ASSOCIATED CONTENT

Supporting Information

The Supporting Information is available free of charge at https://pubs.acs.org/doi/10.1021/acsami.1c19192.

Zeta potential and size stability characterization of the nanoparticles (Figure S1); mouse body weight changes and lung inflammation postvaccination (Figure S2); serum H3-specific antibody titers (Figure S3); ADCC assay results (Figure S4); long-term serum antibody titers against Aic and Phi viruses over six months (Figure S5); inflammatory cytokine levels in infected mice lungs (Figure S6); and comparative analysis of the hemagglutinin (HA) amino acid sequences between different influenza virus strains (Table S1) (PDF)

■ AUTHOR INFORMATION

Corresponding Author

Bao-Zhong Wang − *Center for Inflammation, Immunity & Infection, Georgia State University Institute for Biomedical Sciences, Atlanta, Georgia 30303, United States;* orcid.org/0000-0002-1561-4318; Email: bwang23@gsu.edu

Authors

Chunhong Dong − *Center for Inflammation, Immunity & Infection, Georgia State University Institute for Biomedical Sciences, Atlanta, Georgia 30303, United States;* orcid.org/0000-0001-6950-6120

Ye Wang − *Center for Inflammation, Immunity & Infection, Georgia State University Institute for Biomedical Sciences, Atlanta, Georgia 30303, United States*

Wandi Zhu − *Center for Inflammation, Immunity & Infection, Georgia State University Institute for Biomedical Sciences, Atlanta, Georgia 30303, United States*

Yao Ma − *Center for Inflammation, Immunity & Infection, Georgia State University Institute for Biomedical Sciences, Atlanta, Georgia 30303, United States*

Joo Kim − *Center for Inflammation, Immunity & Infection, Georgia State University Institute for Biomedical Sciences, Atlanta, Georgia 30303, United States*

Lai Wei − *Center for Inflammation, Immunity & Infection, Georgia State University Institute for Biomedical Sciences, Atlanta, Georgia 30303, United States*

Gilbert X. Gonzalez − *Center for Inflammation, Immunity & Infection, Georgia State University Institute for Biomedical Sciences, Atlanta, Georgia 30303, United States*

Complete contact information is available at: https://pubs.acs.org/10.1021/acsami.1c19192

Notes

The authors declare no competing financial interest.

The data necessary for reproducing these findings are available from the corresponding author upon request.

■ ACKNOWLEDGMENTS

The present studies reported were supported by the National Institute of Allergy and Infectious Diseases of the National Institutes of Health (NIAID) of the National Institutes of Health (NIH) under Award Numbers R01AI101047, R01AI116835, and R01AI143844 to B.-Z.W. The content is solely the authors' responsibility and does not necessarily represent the official views of the funder.

■ REFERENCES

(1) Centers for Disease Control and Prevention. *Estimated Influenza Illnesses, Medical visits, Hospitalizations, and Deaths in the United States — 2019−2020 Influenza Season*; https://www.cdc.gov/flu/about/burden/2019-2020.html (accessed: September, 2021).

(2) Chevalier, C.; Calzas, C. Innovative mucosal vaccine formulations against influenza A virus infections. *Front. Immunol.* **2019**, *10*, 1605.

(3) Rose, M. A.; Zielen, S.; Baumann, U. Mucosal immunity and nasal influenza vaccination. *Expert Rev. Vaccines* **2012**, *11* (5), 595−607.

(4) Rajao, D. S.; Perez, D. R. Universal Vaccines and Vaccine Platforms to Protect against Influenza Viruses in Humans and Agriculture. *Front Microbiol.* **2018**, *9*, 123.

(5) Wei, C. J.; Crank, M. C.; Shiver, J.; Graham, B. S.; Mascola, J. R.; Nabel, G. J. Next-generation influenza vaccines: opportunities and challenges. *Nat. Rev. Drug Discov.* **2020**, *19* (4), 239−252.

(6) Sia, Z. R.; Miller, M. S.; Lovell, J. F. Engineered Nanoparticle Applications for Recombinant Influenza Vaccines. *Mol. Pharmaceutics* **2021**, *18* (2), 576−592.

(7) Richards, K. A.; Moritzky, S.; Shannon, I.; Fitzgerald, T.; Yang, H.; Branche, A.; Topham, D. J.; Treanor, J. J.; Nayak, J.; Sant, A. J. Recombinant HA-based vaccine outperforms split and subunit vaccines in elicitation of influenza-specific CD4 T cells and CD4 T cell-dependent antibody responses in humans. *npj Vaccines* **2020**, *5* (1), 77.

(8) Cox, M. M.; Patriarca, P. A.; Treanor, J. FluBlok, a recombinant hemagglutinin influenza vaccine. *Influenza Other Respir. Viruses* **2008**, *2* (6), 211−9.

(9) Huber, V. C.; McKeon, R. M.; Brackin, M. N.; Miller, L. A.; Keating, R.; Brown, S. A.; Makarova, N.; Perez, D. R.; Macdonald, G. H.; McCullers, J. A. Distinct contributions of vaccine-induced immunoglobulin G1 (IgG1) and IgG2a antibodies to protective immunity against influenza. *Clin. Vaccine Immunol.* **2006**, *13* (9), 981−90.

(10) Balkovic, E. S.; Florack, J. A.; Six, H. R. Immunoglobulin G subclass antibody responses of mice to influenza virus antigens given in different forms. *Antiviral Res.* **1987**, *8* (3), 151−60.

(11) Moran, T. M.; Park, H.; Fernandez-Sesma, A.; Schulman, J. L. Th2 responses to inactivated influenza virus can Be converted to Th1 responses and facilitate recovery from heterosubtypic virus infection. *J. Infect. Dis.* **1999**, *180* (3), 579−85.

(12) Wibowo, D.; Jorritsma, S. H. T.; Gonzaga, Z. J.; Evert, B.; Chen, S. X.; Rehm, B. H. A. Polymeric nanoparticle vaccines to combat emerging and pandemic threats. *Biomaterials* **2021**, *268*, 120597.
(13) Zhou, X.; Jiang, X.; Qu, M.; Aninwene, G. E., 2nd; Jucaud, V.; Moon, J. J.; Gu, Z.; Sun, W.; Khademhosseini, A. Engineering Antiviral Vaccines. *ACS Nano* **2020**, *14* (10), 12370−12389.
(14) Feng, X.; Xu, W.; Li, Z.; Song, W.; Ding, J.; Chen, X. Immunomodulatory Nanosystems. *Adv. Sci.* **2019**, *6* (17), 1900101.
(15) Cossette, B.; Kelly, S. H.; Collier, J. H. Intranasal Subunit Vaccination Strategies Employing Nanomaterials and Biomaterials. *ACS Biomater. Sci. Eng.* **2021**, *7* (5), 1765−1779.
(16) Knight, F. C.; Gilchuk, P.; Kumar, A.; Becker, K. W.; Sevimli, S.; Jacobson, M. E.; Suryadevara, N.; Wang-Bishop, L.; Boyd, K. L.; Crowe, J. E., Jr.; Joyce, S.; Wilson, J. T. Mucosal Immunization with a pH-Responsive Nanoparticle Vaccine Induces Protective CD8(+) Lung-Resident Memory T Cells. *ACS Nano* **2019**, *13* (10), 10939−10960.
(17) Wang, B. Z.; Xu, R.; Quan, F. S.; Kang, S. M.; Wang, L.; Compans, R. W. Intranasal immunization with influenza VLPs incorporating membrane-anchored flagellin induces strong heterosubtypic protection. *PLoS One* **2010**, *5* (11), e13972.
(18) Donaldson, B.; Lateef, Z.; Walker, G. F.; Young, S. L.; Ward, V. K. Virus-like particle vaccines: immunology and formulation for clinical translation. *Expert Rev. Vaccines* **2018**, *17* (9), 833−849.
(19) Dong, C.; Wang, Y.; Gonzalez, G. X.; Ma, Y.; Song, Y.; Wang, S.; Kang, S. M.; Compans, R. W.; Wang, B. Z. Intranasal vaccination with influenza HA/GO-PEI nanoparticles provides immune protection against homo- and heterologous strains. *Proc. Natl. Acad. Sci. U. S. A.* **2021**, *118* (19), e2024998118.
(20) Li, S.; Guo, Z.; Zeng, G.; Zhang, Y.; Xue, W.; Liu, Z. Polyethylenimine-Modified Fluorescent Carbon Dots As Vaccine Delivery System for Intranasal Immunization. *ACS Biomater. Sci. Eng.* **2018**, *4* (1), 142−150.
(21) Tao, W.; Hurst, B. L.; Shakya, A. K.; Uddin, M. J.; Ingrole, R. S.; Hernandez-Sanabria, M.; Arya, R. P.; Bimler, L.; Paust, S.; Tarbet, E. B.; Gill, H. S. Consensus M2e peptide conjugated to gold nanoparticles confers protection against H1N1, H3N2 and H5N1 influenza A viruses. *Antiviral Res.* **2017**, *141*, 62−72.
(22) Tao, W. Q.; Gill, H. S. M2e-immobilized gold nanoparticles as influenza A vaccine: Role of soluble M2e and longevity of protection. *Vaccine* **2015**, *33* (20), 2307−2315.
(23) Ingrole, R. S. J.; Tao, W. Q.; Joshi, G.; Gill, H. S. M2e conjugated gold nanoparticle influenza vaccine displays thermal stability at elevated temperatures and confers protection to ferrets. *Vaccine* **2021**, *39* (34), 4800−4809.
(24) Wang, J.; Li, P.; Yu, Y.; Fu, Y.; Jiang, H.; Lu, M.; Sun, Z.; Jiang, S.; Lu, L.; Wu, M. X. Pulmonary surfactant-biomimetic nanoparticles potentiate heterosubtypic influenza immunity. *Science* **2020**, *367* (6480), eaau0810.
(25) Shen, C.; Li, J.; Zhang, Y.; Li, Y. C.; Shen, G. X.; Zhu, J. T.; Tao, J. Polyethylenimine-based micro/nanoparticles as vaccine adjuvants (vol 12, pg 5443, 2017). *Int. J. Nanomed.* **2017**, *12*, 7239−7239.
(26) Wegmann, F.; Gartlan, K. H.; Harandi, A. M.; Brinckmann, S. A.; Coccia, M.; Hillson, W. R.; Kok, W. L.; Cole, S.; Ho, L. P.; Lambe, T.; Puthia, M.; Svanborg, C.; Scherer, E. M.; Krashias, G.; Williams, A.; Blattman, J. N.; Greenberg, P. D.; Flavell, R. A.; Moghaddam, A. E.; Sheppard, N. C.; Sattentau, Q. J. Polyethyleneimine is a potent mucosal adjuvant for viral glycoprotein antigens. *Nat. Biotechnol.* **2012**, *30* (9), 883−8.
(27) Marichal, T.; Ohata, K.; Bedoret, D.; Mesnil, C.; Sabatel, C.; Kobiyama, K.; Lekeux, P.; Coban, C.; Akira, S.; Ishii, K. J.; Bureau, F.; Desmet, C. J. DNA released from dying host cells mediates aluminum adjuvant activity. *Nat. Med.* **2011**, *17* (8), 996−1002.
(28) Doherty, P. C.; Turner, S. J.; Webby, R. G.; Thomas, P. G. Influenza and the challenge for immunology. *Nat. Immunol.* **2006**, *7* (5), 449−55.
(29) Jin, J. W.; Tang, S. Q.; Rong, M. Z.; Zhang, M. Q. Synergistic effect of dual targeting vaccine adjuvant with aminated beta-glucan and CpG-oligodeoxynucleotides for both humoral and cellular immune responses. *Acta Biomater.* **2018**, *78*, 211−223.
(30) Hayashi, T.; Momota, M.; Kuroda, E.; Kusakabe, T.; Kobari, S.; Makisaka, K.; Ohno, Y.; Suzuki, Y.; Nakagawa, F.; Lee, M. S. J.; Coban, C.; Onodera, R.; Higashi, T.; Motoyama, K.; Ishii, K. J.; Arima, H. DAMP-Inducing Adjuvant and PAMP Adjuvants Parallelly Enhance Protective Type-2 and Type-1 Immune Responses to Influenza Split Vaccination. *Front Immunol.* **2018**, *9*, 2619.
(31) Shirota, H.; Klinman, D. M. Recent progress concerning CpG DNA and its use as a vaccine adjuvant. *Expert Rev. Vaccines* **2014**, *13* (2), 299−312.
(32) de Titta, A.; Ballester, M.; Julier, Z.; Nembrini, C.; Jeanbart, L.; van der Vlies, A. J.; Swartz, M. A.; Hubbell, J. A. Nanoparticle conjugation of CpG enhances adjuvancy for cellular immunity and memory recall at low dose. *Proc. Natl. Acad. Sci. U. S. A.* **2013**, *110* (49), 19902−19907.
(33) Shirai, S.; Shibuya, M.; Kawai, A.; Tamiya, S.; Munakata, L.; Omata, D.; Suzuki, R.; Aoshi, T.; Yoshioka, Y. Lipid Nanoparticles Potentiate CpG-Oligodeoxynucleotide-Based Vaccine for Influenza Virus. *Front Immunol.* **2020**, *10*, 3018.
(34) Weldon, W. C.; Wang, B.-Z.; Martin, M. P.; Koutsonanos, D. G.; Skountzou, I.; Compans, R. W. Enhanced immunogenicity of stabilized trimeric soluble influenza hemagglutinin. *PLoS One* **2010**, *5* (9), e12466.
(35) Vyas, S. P.; Gupta, P. N. Implication of nanoparticles/microparticles in mucosal vaccine delivery. *Expert Rev. Vaccines* **2007**, *6* (3), 401−18.
(36) Van den Hoecke, S.; Ehrhardt, K.; Kolpe, A.; El Bakkouri, K.; Deng, L.; Grootaert, H.; Schoonooghe, S.; Smet, A.; Bentahir, M.; Roose, K.; Schotsaert, M.; Schepens, B.; Callewaert, N.; Nimmerjahn, F.; Staeheli, P.; Hengel, H.; Saelens, X. Hierarchical and Redundant Roles of Activating FcgammaRs in Protection against Influenza Disease by M2e-Specific IgG1 and IgG2a Antibodies. *J. Virol.* **2017**, *91* (7), e02500−16.
(37) Wang, X.; Yang, D.; Li, S.; Xu, X.; Qin, C. F.; Tang, R. Biomineralized vaccine nanohybrid for needle-free intranasal immunization. *Biomaterials* **2016**, *106*, 286−94.
(38) Mozdzanowska, K.; Furchner, M.; Washko, G.; Mozdzanowski, J.; Gerhard, W. A pulmonary influenza virus infection in SCID mice can be cured by treatment with hemagglutinin-specific antibodies that display very low virus-neutralizing activity in vitro. *J. Virol.* **1997**, *71* (6), 4347−55.
(39) Gerhard, W.; Mozdzanowska, K.; Furchner, M.; Washko, G.; Maiese, K. Role of the B-cell response in recovery of mice from primary influenza virus infection. *Immunol. Rev.* **1997**, *159*, 95−103.
(40) Jegaskanda, S.; Reading, P. C.; Kent, S. J. Influenza-specific antibody-dependent cellular cytotoxicity: toward a universal influenza vaccine. *J. Immunol.* **2014**, *193* (2), 469−75.
(41) Vanderven, H. A.; Kent, S. J. The protective potential of Fc-mediated antibody functions against influenza virus and other viral pathogens. *Immunol. Cell Biol.* **2020**, *98* (4), 253−263.
(42) DiLillo, D. J.; Tan, G. S.; Palese, P.; Ravetch, J. V. Broadly neutralizing hemagglutinin stalk-specific antibodies require FcgammaR interactions for protection against influenza virus in vivo. *Nat. Med.* **2014**, *20* (2), 143−51.
(43) La Gruta, N. L.; Turner, S. J. T cell mediated immunity to influenza: mechanisms of viral control. *Trends Immunol.* **2014**, *35* (8), 396−402.
(44) Altenburg, A. F.; Rimmelzwaan, G. F.; de Vries, R. D. Virus-specific T cells as correlate of (cross-)protective immunity against influenza. *Vaccine* **2015**, *33* (4), 500−6.
(45) Bot, A.; Bot, S.; Bona, C. A. Protective role of gamma interferon during the recall response to influenza virus. *J. Virol.* **1998**, *72* (8), 6637−45.
(46) Grant, E. J.; Quinones-Parra, S. M.; Clemens, E. B.; Kedzierska, K. Human influenza viruses and CD8(+) T cell responses. *Curr. Opin. Virol.* **2016**, *16*, 132−142.

https://doi.org/10.1021/acsami.1c19192
ACS Appl. Mater. Interfaces 2022, 14, 6331−6342

(47) Brown, D. M.; Lee, S.; Garcia-Hernandez, M. L.; Swain, S. L. Multifunctional CD4 cells expressing gamma interferon and perforin mediate protection against lethal influenza virus infection. *J. Virol.* **2012**, *86* (12), 6792−6803.
(48) Chen, J.; Li, Z.; Huang, H.; Yang, Y.; Ding, Q.; Mai, J.; Guo, W.; Xu, Y. Improved antigen cross-presentation by polyethyleneimine-based nanoparticles. *Int. J. Nanomedicine* **2011**, *6*, 77−84.
(49) Emami, A.; Tepper, J.; Short, B.; Yaksh, T. L.; Bendele, A. M.; Ramani, T.; Cisternas, A. F.; Chang, J. H.; Mellon, R. D. Toxicology Evaluation of Drugs Administered via Uncommon Routes: Intranasal, Intraocular, Intrathecal/Intraspinal, and Intra-Articular. *Int. J. Toxicol.* **2018**, *37* (1), 4−27.
(50) Keller, L. A.; Merkel, O.; Popp, A. Intranasal drug delivery: opportunities and toxicologic challenges during drug development. *Drug Deliv. Transl. Res.* **2021**, DOI: 10.1007/s13346-020-00891-5.
(51) Wang, C.; Zhu, W.; Luo, Y.; Wang, B.-Z. Gold nanoparticles conjugating recombinant influenza hemagglutinin trimers and flagellin enhanced mucosal cellular immunity. *Nanomedicine: NBM* **2018**, *14* (4), 1349−1360.
(52) Creanga, A.; Gillespie, R. A.; Fisher, B. E.; Andrews, S. F.; Lederhofer, J.; Yap, C.; Hatch, L.; Stephens, T.; Tsybovsky, Y.; Crank, M. C.; Ledgerwood, J. E.; McDermott, A. B.; Mascola, J. R.; Graham, B. S.; Kanekiyo, M. A comprehensive influenza reporter virus panel for high-throughput deep profiling of neutralizing antibodies. *Nat. Commun.* **2021**, *12* (1), 1722.
(53) Wang, Y.; Deng, L.; Gonzalez, G. X.; Luthra, L.; Dong, C.; Ma, Y.; Zou, J.; Kang, S. M.; Wang, B. Z. Double-Layered M2e-NA Protein Nanoparticle Immunization Induces Broad Cross-Protection against Different Influenza Viruses in Mice. *Adv. Healthcare Mater.* **2020**, *9* (2), 1901176.

https://doi.org/10.1021/acsami.1c19192
ACS Appl. Mater. Interfaces 2022, 14, 6331−6342